TÜBİTAK

Turkish Journal of Biology

http://journals.tubitak.gov.tr/biology/

Research Article

Turk J Biol
(2017) 41: 719-733
© TÜBİTAK
doi:10.3906/biy-1612-17

Targeted delivery of etoposide to osteosarcoma cells using poly(3-hydroxybutyrate-co-3-hydroxyvalerate) (PHBV) nanoparticles

Esma ALP[1], Tamer ÇIRAK[1,2], Murat DEMİRBİLEK[1], Mustafa TÜRK[3], Eylem GÜVEN[1,*]

[1]Nanotechnology and Nanomedicine Division, Hacettepe University, Ankara, Turkey

[2]Alternative Energy Sources Division, Vocational School of Technical Sciences, Aksaray University, Aksaray, Turkey

[3]Department of Bioengineering, Faculty of Engineering, Kırıkkale University, Kırıkkale, Turkey

Received: 09.12.2016 • **Accepted/Published Online:** 11.02.2017 • **Final Version:** 10.11.2017

Abstract: Folic acid (FA)-functionalized poly(3-hydroxybutyrate-co-3-hydroxyvalerate) (PHBV) nanoparticles were prepared to enhance the delivery efficiency of the anticancer drug etoposide for the clinical treatment of osteosarcoma. PHBV nanoparticles were synthesized by emulsification/solvent evaporation technique and obtained in the size range of 200–250 nm and zeta potential range of –21 and –27 mV. Encapsulation efficiency and in vitro drug release were studied. The cytotoxic, apoptotic, and necrotic effects of PHBV nanoparticles were also investigated using Saos-2 osteosarcoma cells. The results obtained in this study demonstrate that etoposide-loaded and FA-functionalized PHBV nanoparticles can be successfully used for targeted treatment of osteosarcoma.

Key words: PHBV nanoparticle, folate targeting, etoposide, targeted drug delivery, osteosarcoma

1. Introduction

Osteosarcoma (OS), or osteogenic sarcoma, is the most common primary bone tumor in children and adolescents, accounting for 5% of all pediatric malignancies. It is a high-grade neoplasm with rapid growth and early metastasis, which typically is pulmonary. Current major OS therapy options include combinations of surgery and chemotherapy. Various chemotherapeutic agents, such as doxorubicin, methotrexate, cyclophosphamide, etoposide, and cisplatin, are commonly used, either alone or in combination (Wittig et al., 2002). Although the 5-year survival rate is 15% to 20% for patients with localized osteosarcoma with surgery alone, it increases dramatically to approximately 70% in combination with chemotherapy. However, the eventual development of multidrug resistance to multiple types of chemotherapeutic agents hampers the efficacy of chemotherapy. It is estimated that less than 30% of patients with recurrent disease will be cured (Schwartz et al., 2007). Therefore, more effective therapeutic agents with higher specificity and lower toxicity are needed to overcome the dose-limiting side effects of conventional chemotherapeutic agents and therapeutic failure due to multidrug resistant tumor cells.

An effective approach to improving the therapeutic indices of anticancer agents is the development of targeted drug delivery systems utilizing nanotechnological strategies. Nanoparticles have the potential to deliver chemotherapeutic agents to targeted cells and make therapeutic delivery procedures more effective, more precise, and less harmful to healthy tissues (Jabir et al., 2012). Polymeric nanoparticles have attracted much attention as drug delivery systems based on their ease of preparation and ability to tailor their properties for the design of suitable targeted drug delivery systems with required characteristics (Parveen and Sahoo, 2008). To improve nanoparticular drug delivery, active targeting is widely used. In active targeting, nanoparticles are chemically modified with different ligands that precisely recognize and specifically interact with receptors on targeted cells (Yu et al., 2012).

Folate receptors are highly specific tumor markers overexpressed in many human cancer types, including ovarian cancer, choriocarcinomas, uterine sarcomas, and osteocarcinomas (Vasir and Labhasetwar, 2005). They have gained considerable attention for targeted drug delivery. Folic acid has been frequently used to specifically target attached chemotherapeutic agents to tumor cells that overexpress folate receptors (Low and Kularatne, 2009). Functionalization of nanoparticles with folic acid significantly enhances the internalization and binding affinity of the nanoparticles toward folate receptor overexpressed cells.

* Correspondence: eylemoz@hacettepe.edu.tr

Etoposide, a derivative of podophyllotoxin, is an antineoplastic drug used to treat various human cancer types, such as lung cancer, lymphomas, Ewing's sarcoma, ovarian cancer, and osteosarcoma (Hande, 1998). Etoposide, the most frequently prescribed chemotherapeutic agent currently used for the treatment of human cancers, induces DNA damage by inhibition of topoisomerase II. However, etoposide has poor solubility in water, limited chemical and physical stability, and side effects on patients. In order to eliminate these problems, particulate drug delivery systems have been used (Dhanaraju et al., 2010; Zhang et al., 2011).

Polyhydroxyalkanoates (PHAs), synthesized by a variety of microorganisms, are a class of naturally occurring biodegradable and biocompatible polyesters. They have gained significant attention as drug delivery materials due to their promising physicochemical and mechanical properties. Poly(3-hydroxybutyrate) (PHB) is the first and the most extensively studied member of the PHA family. However, PHB has brittleness and low mechanical strength, which makes it restricted for these applications. On the other hand, the poor low-impact strength of PHB is eliminated by incorporating hydroxyvalerate monomers into the polymer chain to produce polyhydroxybutyrate-co-valerate (PHBV). The addition of polyhydroxyvalerate (PHV) to the PHB polymer chain in varying ratios reduces crystallinity and makes it more flexible and more easily processable than PHB itself (Gassner and Owen, 1996).

In the present study, we developed PHBV nanoparticles for the targeted delivery of etoposide to osteosarcoma cells. Folic acid was used as the targeting ligand to take advantage of folate-receptor–mediated endocytosis. Obtained nanoparticles were characterized using zeta sizer, zeta potential, FT–IR, and scanning electron microscopy. In vitro etoposide release and encapsulation efficiency were investigated. Furthermore, the delivery system was evaluated for cytotoxicity using an MTT-based assay. Apoptosis and necrosis indices were also evaluated. The cytotoxic, apoptotic, and necrotic effects of PHBV nanoparticles were investigated using the folate-receptor–overexpressing Saos-2 osteosarcoma cells.

2. Materials and methods

PHBV (8% 3-hydroxyvalerate, Mw = 150,000), 3-(4,5-dimethylthiazol)-2,5-diphenyltetrazolium bromide, folic acid, 1-ethyl-3-(3-dimethyl-aminopropyl) carbodiimide (EDAC), and MES were purchased from Sigma Aldrich (St. Louis, MO, USA). Etoposide was purchased from Ebewe Pharma (Unterach, Austria). Chloroform, ethyl alcohol, and Tween 80 were purchased from Merck (Darmstadt, Germany). Trypsin-EDTA, D-MEM/F-12, FCS, DMSO, penicillin–streptomycin, RPMI 1640 medium, and L-glutamine were purchased from Biological Industries (Beit-Haemek, Israel). Hoechst 33342 and propidium iodide were purchased from Serva (Abu-Gosh, Israel). Annexin-V-FLUOS was purchased from Roche (Indianapolis, IN, USA).

2.1. Preparation of PHBV nanoparticles

PHBV nanoparticles were prepared by an emulsification/solvent evaporation technique adapted from previously described methods (Vilos et al., 2013). Briefly, 10 mg of PHBV was dissolved in 10 mL of chloroform to obtain 0.1% (w/v) organic phase. The organic phase was injected into an aqueous phase containing 6% (w/v) Tween 80/distilled water with a syringe in a high-speed homogenizer at 24,000 rpm (Ultra-Turrax, T18 basic, IKA; Staufen im Breisgau, Germany) in an inert nitrogen-filled environment. The organic solvent was allowed to volatilize while the nanoparticles formed under continuous mechanical stirring at room temperature for 2 h. PHBV nanoparticles were collected following centrifugation at 12,000 rpm for 30 min and washed three times with distilled water. Drug-loaded nanoparticles were prepared using the same method, except that PHBV and etoposide were dissolved in chloroform at different polymer/drug ratios (w/w) (1/1, 1/0.5, 1/0.25) prior to emulsification (Table 1). Obtained nanoparticles were lyophilized using a freeze dryer.

2.2. Fabrication of folic-acid–conjugated PHBV nanoparticles

Folic-acid–conjugated PHBV nanoparticles were synthesized by carbodiimide method (Kilicay et al., 2011). Folic acid was attached to PHBV nanoparticles through the formation of an amide linkage between the carboxyl group of PHBV and the amine group of folic acid using EDAC. Briefly, 1.0 mg/mL folic acid solution was prepared in 1.0 mL of water by adjusting the pH to weak alkaline. Folate-attached PHBV nanoparticles were obtained by the addition of folate solution into the activated 10.0 mL of PHBV nanoparticle suspension (1.0 mg/mL) corresponding to a PHBV:EDAC weight ratio of 1:1 and 2 h of activation time. The mixture was stirred at room temperature for 24 h. The nanoparticle suspension was centrifuged at 12,000 rpm for 30 min and the supernatants were stored for further analysis. Nanoparticles were washed with distilled water and freeze-dried to get the nanoparticle powder. The quantity of unconjugated folic acid remaining in the supernatant was determined using a UV–Vis spectrophotometer (NanoDrop ND-1000, Thermo Scientific; Waltham, MA, USA) by measuring the UV absorbance at $\lambda = 280$ nm.

2.3. Characterization of PHBV nanoparticles

SEM (ESEM, FEI Quanta; Houston, TX, USA) was used to examine the nanoparticle morphologies. FTIR analysis was carried out for the structural characterization of nanoparticles (Shimadzu, DR8101; Kyoto, Japan). All size

and size distribution parameters were measured according to dynamic light scattering measurements (DLS) using a Zetasizer nanoparticle analyzer (Malvern Instruments, Model 3000 HSA; Malvern, UK). The particle size and polydispersity index (PdI) for each sample were measured twice and the average value was reported. The zeta potential values were determined using a Zetasizer nanoparticle analyzer.

2.4. Determination of entrapment efficiency

Nanoparticles at different initial polymer/drug ratios (w/w) (i.e. 1/1, 1/0.5, and 1/0.25) were dissolved in chloroform for the extraction of the drug from nanoparticles and the amount of drug in the solution was measured using a UV–Vis spectrophotometer (NanoDrop ND-1000, Thermo Scientific) at a wavelength of 284 nm. The entrapment efficiency (EE) was then calculated using Eq. (1):

$$EE\ \% = \frac{\text{weight of drug in nanoparticles}}{\text{initial weight of drug used in the formulation}} \times 100\% \quad (1)$$

2.5. In vitro etoposide release studies

The in vitro release studies of PHBV nanoparticles were carried out at 37 °C in phosphate-buffered saline (PBS, pH 7.4). Typically, 5 mL of PBS was added into two compartments separated by a dialysis membrane, and 50 mg of PHBV nanoparticles at different initial polymer/drug ratios (w/w) (1/1, 1/0.5, 1/0.25) were added to one of the compartments. The entire system was kept at 37 °C by gentle shaking in a water bath. Samples (0.2 mL) were removed from the receptor compartment at predetermined time intervals and replaced with the same volume of fresh buffer. The amount of free etoposide released from the nanoparticles was measured using a UV–Vis spectrophotometer at a wavelength of 284 nm (NanoDrop ND-1000, Thermo Scientific). Experiments were carried out in triplicate.

2.6. Cytotoxicity assay

The cellular toxicity of blank PHBV nanoparticles as well as nontargeted and folic-acid–targeted PHBV nanoparticles at different initial polymer/drug ratios (1/1, 1/0.5, and 1/0.25) and nanoparticle concentrations (5, 10, 25, and 50 μg/mL) were determined by using the Saos-2 osteosarcoma cell line. Free etoposide at various concentrations (5, 10, 25, and 50 μg/mL) was also tested. The cells were cultured in DMEM/F-12 medium supplemented with 10% FBS and 1% penicillin–streptomycin. A total of 5×10^3 cells were seeded in 96-well plates. After incubation at 37 °C in a 5% CO_2-humidified incubator overnight, the medium was discarded and plates were washed with buffer solution. Subsequently cells were treated with samples of increasing concentrations (5, 10, 25, and 50 μg/mL) for 24 h and 48 h. The cell viabilities at given time intervals were measured using MTT (3-(4,5-dimethylthiazole-2-yl)-2,5-diphenyl tetrazolium) assay, which monitors the mitochondrial metabolism of cells as an indicator of viability (van Meerloo et al., 2011). Briefly, 100 μL of MTT reagent (5.0 mg/mL, diluted with RPMI 1640 without phenol red, filtered through a 0.22-μm filter) was added to each well after the cells were washed with buffer solution to remove noninternalized nanoparticles. After 4 h of incubation (37 °C and 5% CO_2), the medium was removed and 100 μL of isopropanol with 0.04 N HCl was added to each well to ensure solubilization of formazan crystals by shaking at 240 rpm for 10 min. Finally, the absorbance was determined using an ELISA plate reader (ASYS Expert Plus ELISA reader, Biochrom Ltd.; Cambourne, UK) at 570 nm. Cytotoxicity studies were performed in triplicate and the data were represented as mean ± standard deviation (SD).

2.7. Apoptosis/necrosis assay

Apoptosis-mediated cell death of tumor cells induced by PHBV nanoparticle formulations were analyzed by using Hoechst–propidium iodide double-staining and Annexin V–propidium iodide double-staining methods.

2.7.1. Hoechst–propidium iodide double staining

Saos-2 cells were seeded in 48-well cell culture plates at a density of 1×10^4 cells/well in DMEM-F12 medium supplemented with 10% fetal bovine serum and 1% penicillin–streptomycin at 37 °C in a humidified 5% CO_2 atmosphere. The cells were then treated with free etoposide, nontargeted PHBV nanoparticles, and folic-acid–attached PHBV nanoparticles (polymer/drug ratio; (1/1, 1/0.5, 1/0.25). Increasing concentrations (5, 10, 25, and 50 μg/mL) of samples were incubated with the cells. Untreated cells and blank nanoparticle-treated cells were used as controls. Following 24 h of treatment, cells were collected and washed with PBS. Cells were stained with Hoechst 33342 nucleic acid dye (2 μg/mL), propidium iodide (2 μg/mL), and DNAse free-RNAse (100 μg/mL) for 15 min at room temperature. The number of apoptotic and necrotic cells were determined by inverted fluorescence microscope (Leica DM6000, Leica Microsystems; Wetzlar, Germany). The number of apoptotic and necrotic cells in 10 randomly chosen microscopic fields were counted and the results were expressed as a ratio of apoptotic and necrotic cells to normal cells. The data are represented as means ± SD.

2.7.2. Annexin V–propidium iodide double staining

Saos-2 cells were treated with a medium containing free etoposide, nontargeted PHBV nanoparticles, and folic-acid–attached PHBV nanoparticles at increasing concentrations (5, 10, 25, and 50 μg/mL) of samples. Nontreated cells were used as the control. Following the treatment, adherent cells were collected, washed in PBS, and resuspended in binding buffer (10 mM HEPES/NaOH, pH: 7.4, 140 mM NaCl, 2.5 mM $CaCl_2$). Annexin V and propidium iodide were added to a final concentration of 10 μg/mL and 1 μg/

mL, respectively, and the cells were incubated in darkness for 10 min. The number of Annexin V-labeled cells was counted using an inverted fluorescence microscope (Leica DM6000, Leica Microsystems). For each image (at least 100 cells/field) three randomly selected microscopic fields were evaluated. The data are represented as means ± SD.

3. Results and discussion

3.1. Characterization of nanoparticles

3.1.1. Morphological characterization of nanoparticles

The morphological image of PHBV nanoparticles obtained by SEM is shown in Figure 1. Obtained nanoparticles had a spherical shape and were homogeneously distributed with narrow size distribution.

3.1.2. FTIR analysis of folic-acid–conjugated PHBV nanoparticles

The surface functionalization of PHBV nanoparticles was confirmed by FTIR (Figure 2). As seen in Figure 2C, the absorption bands at 3335 cm^{-1} and 1635 cm^{-1} correspond to the NH– stretching and C=O stretching vibrations of the $–CONH_2$ group, indicating a coupling reaction between the folic acid and the PHBV nanoparticle through the amide linkage (Zhang et al., 2010). Additionally, the folic-acid–conjugated PHBV had an adsorption peak at 1462 cm^{-1} assigned to the stretching vibrations of C=C in the backbone of the aromatic ring of folic acid (Xu et al., 2016).

3.1.3. Particle size and zeta potential

The biological fate of nanoparticles and the interaction of nanoparticles with cells depend on several key parameters, including size, surface charge, cell type, and the modification of the nanoparticles (Decuzzi and Ferrari, 2007). These factors affect drug release rate, pharmacokinetics and biodistribution of the nanoparticles, cellular uptake, and therapeutic effect of encapsulated drugs. Studies have demonstrated that the smaller size of polymeric nanoparticles can reduce the reticuloendothelial system clearance, prolonging the time of circulation of nanoparticles in the bloodstream, thus resulting in high intracellular uptake (van Engeland et al., 1998). In this study, the nanoparticle size–size distribution had been optimized by changing the polymer concentration, homogenization rate, and emulsifier concentration.

The dispersed and continuous phase viscosities alter the efficiency of particle size during the formation of nanoparticles (Qian and McClements, 2011). The increase in polymer concentration resulted in larger nanoparticle size due to the increase in the viscosity of the polymer. It can be postulated that the dispersion of the polymer becomes difficult and this factor contributes to the larger particle size (Table 1).

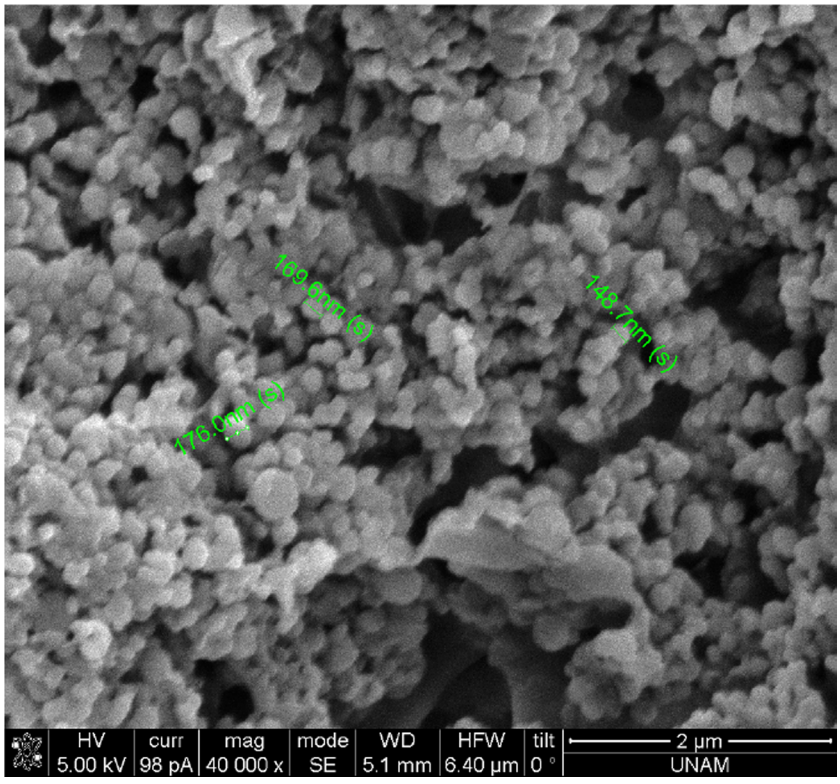

Figure 1. SEM image of PHBV nanoparticles.

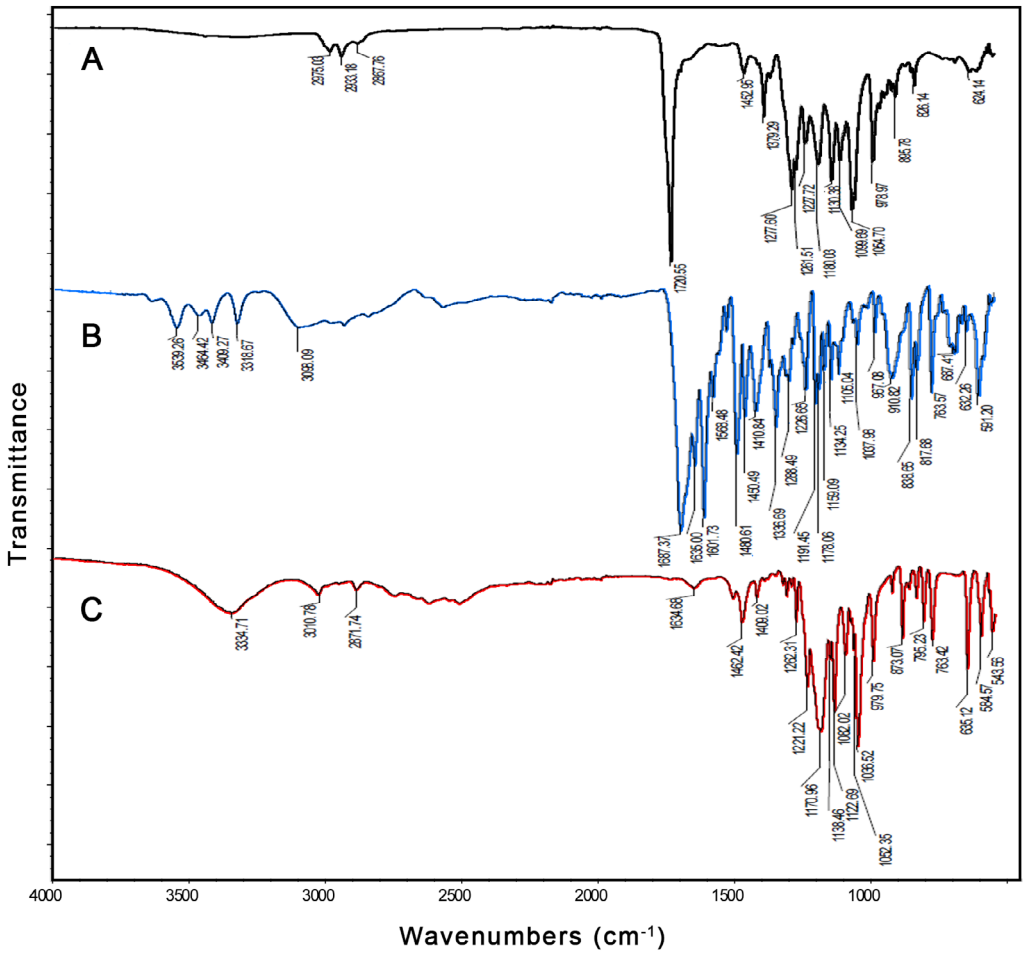

Figure 2. FTIR spectra of (A) PHBV nanoparticle, (B) folic acid (pure), (C) folic-acid–conjugated PHBV nanoparticle.

Table 1. Effect of polymer concentration, emulsifier concentration, and homogenization rate on particle size and polydispersity index.

Sample no.	PHBV/chloroform (mg/mL)	Tween80/dH_2O (mL/mL)	Homogenization rate (rpm)	Particle size (nm ± SD)	Polydispersity index (PDI)
1	0.5	0.05	24,000	210 ± 10	0.133
2	1	0.05	24,000	232 ± 8	0.165
3	2	0.05	24,000	430 ± 15	0.172
4	0.5	0.03	24,000	347 ± 15	0.169
5	0.5	0.01	24,000	650 ± 20	0.192
6	0.5	0.05	7000	622 ± 25	0.227
7	0.5	0.05	15,500	540 ± 20	0.215

The effect of homogenization rate on size and size distribution was determined by using various homogenization rates (7000–24000 rpm) and the results obtained are shown in Table 1. The size of nanoparticles decreased clearly with the increase in the rate of homogenization, as confirmed by previous studies

(Tcholakova et al., 2003; Tan and Nakajima, 2005). The stirring speed is a key factor during the emulsification stage to obtain smaller particle size due the high shear force (Baena-Aristizabal et al., 2016).

Tween 80 acted as a stabilizer in the external aqueous phase and the concentration of Tween 80 played an important role in determining the size of the nanoparticles. It caused a decrease in surface tension difference between the organic and aqueous phases. As seen in Table 1, the increase in emulsifier concentration significantly reduced particle size. This trend was expected because an increased amount of emulsifier caused a rapidly forming layer of emulsifier molecules for the new particle surfaces formed during homogenization process (Qian and McClements, 2011).

As a result of these optimization studies, optimum drug-targeting–applicable nanoparticles were obtained around 210 nm in diameter with a PdI of 0.133, confirmed by dynamic light scattering measurement (Figure 1; Tables 1 and 2). This optimum formulation was used for ligand-binding, drug loading/release, cytotoxicity, and apoptosis/necrosis studies.

Table 2 shows the size–size distribution and zeta potential of the different formulations of PHBV nanoparticles used for cytotoxicity and apoptosis/necrosis studies. The size–size distribution of the prepared nanoparticles was observed to be varied between 200 nm and 250 nm, depending on folic acid modification and etoposide loading. PHBV nanoparticles exhibited a negative surface charge in the range of –21 and –27 mV. As shown in Table 2, the observed values confirm that the zeta potentials of nanoparticles were not greatly affected by increasing amount of etoposide content. For the folic-acid–attached nanoparticles, no significant change was found for the surface charge, despite the carboxylic acid group of folic acid. The results are consistent with other studies on folate-conjugated nanocarriers (Park et al., 2005). The presence of a negative charge on PHBV nanoparticles is a useful characteristic of nanoparticles for improving targeting efficiency. This negative charge reduces the protein-binding affinity of drug-loaded nanoparticles, prolonging the duration at which they remain in circulation without inducing an immune response (Vilos et al., 2013). Patil et al. demonstrated that the positively charged nanoparticles were found to adsorb more bovine serum albumin, while nanoparticles with negative zeta potential had less protein adsorption (Patil et al., 2007).

3.2. Etoposide loading and release studies

With an increase in the initial feeding amount of etoposide from 1/0.25 to 1/1, the encapsulation efficiency of PHBV nanoparticles decreased from 34% to 27%. This result can be explained by the enlarged concentration gradient of drug between the nanoparticle and the outer aqueous phase, which caused more drug loss in the nanoparticle preparation procedure and, in turn, a decrease in encapsulation efficiency of PHBV nanoparticles (Lu et al., 2010). PHBV nanoparticles with an initial polymer/drug ratio of 1/0.5 resulted in 29% encapsulation efficiency.

The drug release profile of nanoparticles loaded with different amounts of drug is shown in Figure 3. The release from a polymeric nanoparticle matrix system, in which the drug is uniformly embedded, generally occurs through a combination of diffusion and degradation of the matrix. The initial drug burst dominates the early release phase, followed by a slow fall in the release rate. The initial fast

Table 2. Data showing the size and zeta potentials of different formulations of nanoparticles.

Nanoparticles	Size (nm)	Polydispersity (PDI)	Zeta potential (mV)
PHBV-NPs	210 ± 10	0.133	–27.2
PHBV-Eto-NPs[a]	212 ± 15	0.145	–25.6
PHBV-Eto-NPs[b]	214 ± 20	0.147	–25.2
PHBV-Eto-NPs[c]	217 ± 12	0.150	–24.9
FA-PHBV-NPs	219 ± 18	0.162	–23.7
FA-PHBV-Eto-NPs[a]	221 ± 20	0.166	–22.6
FA-PHBV-Eto-NPs[b]	223 ± 24	0.169	–21.8
FA-PHBV-NPs[c]	225 ± 30	0.174	–21.1

[a]1/0.25 PHBV/etoposide
[b]1/0.5 PHBV/etoposide
[c]1/1 PHBV/etoposide

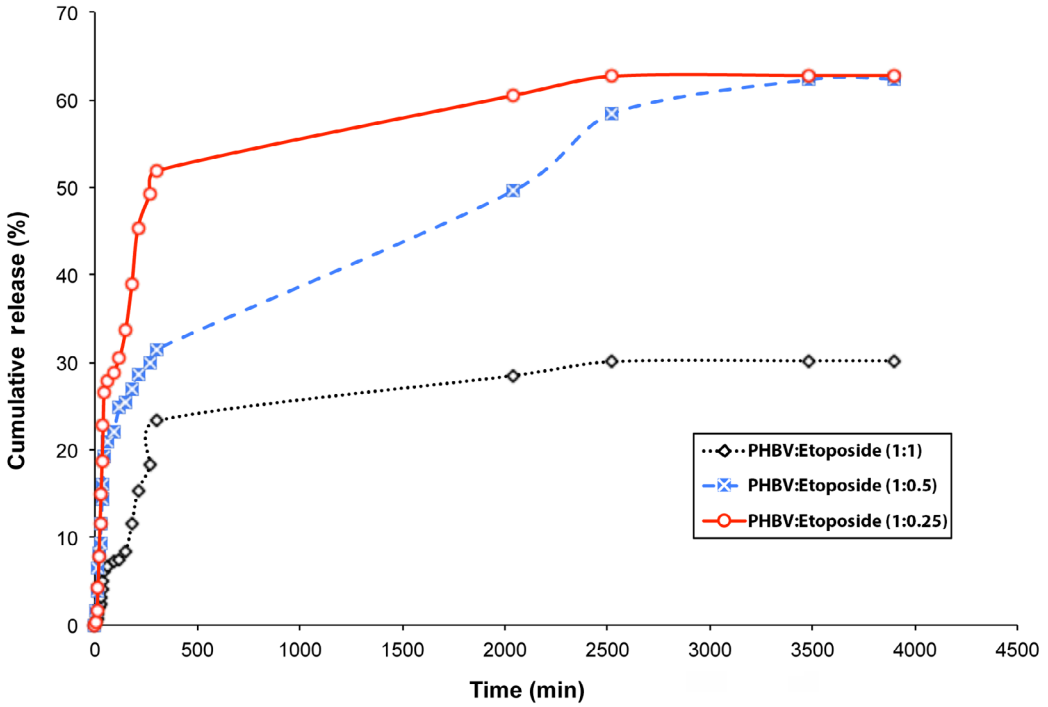

Figure 3. Effect of PHBV/etoposide ratio (w/w) on cumulative etoposide release over time.

drug release is due to the drug being located on or near the particle surface, which diffuses faster to the media, resulting in higher drug release, while a decline in the extent of drug release can be explained by the fact that a higher proportion of accumulation of etoposide within particles restricts the diffusion of drug to the aqueous phase (Bajpai and Mishra, 2005).

3.3. In vitro cytotoxicity studies

Blank PHBV nanoparticles had no significant cytotoxic effect on Saos-2 cells, indicating the safety of the prepared nanoparticles for human use. The viability of Saos-2 cells decreased with the increase in drug concentration of nontargeted nanoparticles and incubation time. After 24 h incubation, 23.6 ± 10.7%, 22.1 ± 10.0%, and 16.3 ± 8.8.% cell mortality was observed for 50 µg/mL of nontargeted nanoparticles at 1/1, 1/0.5, and 1/0.25 initial polymer/drug ratios, respectively. After 48 h incubation, 37.7 ± 8.6%, 26.2 ± 9.0%, and 28.5 ± 9.2% cell mortality was observed for 50 µg/mL of nontargeted nanoparticles at 1/1, 1/0.5, and 1/0.25 initial polymer/drug ratios, respectively (Figures 4A and 4B).

The toxicity of folic-acid–conjugated nanoparticles was also significantly higher than that of nontargeted nanoparticles. Moreover, cell viability decreased with the increase in drug concentration as well as incubation time for targeted nanoparticles (Figures 4A and 4B). For 24 h incubation, folic-acid–conjugated 50 µg/mL PHBV nanoparticles at 1/1, 1/0.5, and 1/0.25 initial polymer/drug ratios resulted in 37.8 ± 6.1%, 23.2 ± 10.01%, and 19.7 ± 5.4% cell mortality, respectively. After 48 h incubation, folic-acid–conjugated 50 µg/mL PHBV nanoparticles at 1/1, 1/0.5, and 1/0.25 initial polymer/drug ratios caused 43.2 ± 4.3%, 38.5 ± 9.8%, and 35.9 ± 5.6% cell mortality, respectively. The overexpression of folate receptors on the surface of Saos-2 cells may significantly enhance the uptake of the targeted nanoparticles via folate-receptor–mediated endocytosis and therefore targeted nanoparticles cause higher cytotoxicity than nontargeted nanoparticles (Yang et al., 2007).

Free etoposide at various concentrations (5–50 µg/mL) was also tested by MTT assay on Saos-2 cells. Higher drug concentrations and incubation times caused lower cell viability. However, a nonsignificant decrease in mortality was observed (Figure 4C).

The results revealed that all the nanoparticle formulations exhibited typical time-dependent and concentration-dependent cytotoxicity. Cytotoxicity was also observed to be highly affected by folic acid conjugation. The results obtained from the in vitro cytotoxicity assay confirmed the enhanced efficacy and higher cytotoxic effect of etoposide loaded and targeted PHBV nanoparticles as compared with etoposide-loaded and nontargeted PHBV nanoparticles, as well as pure etoposide.

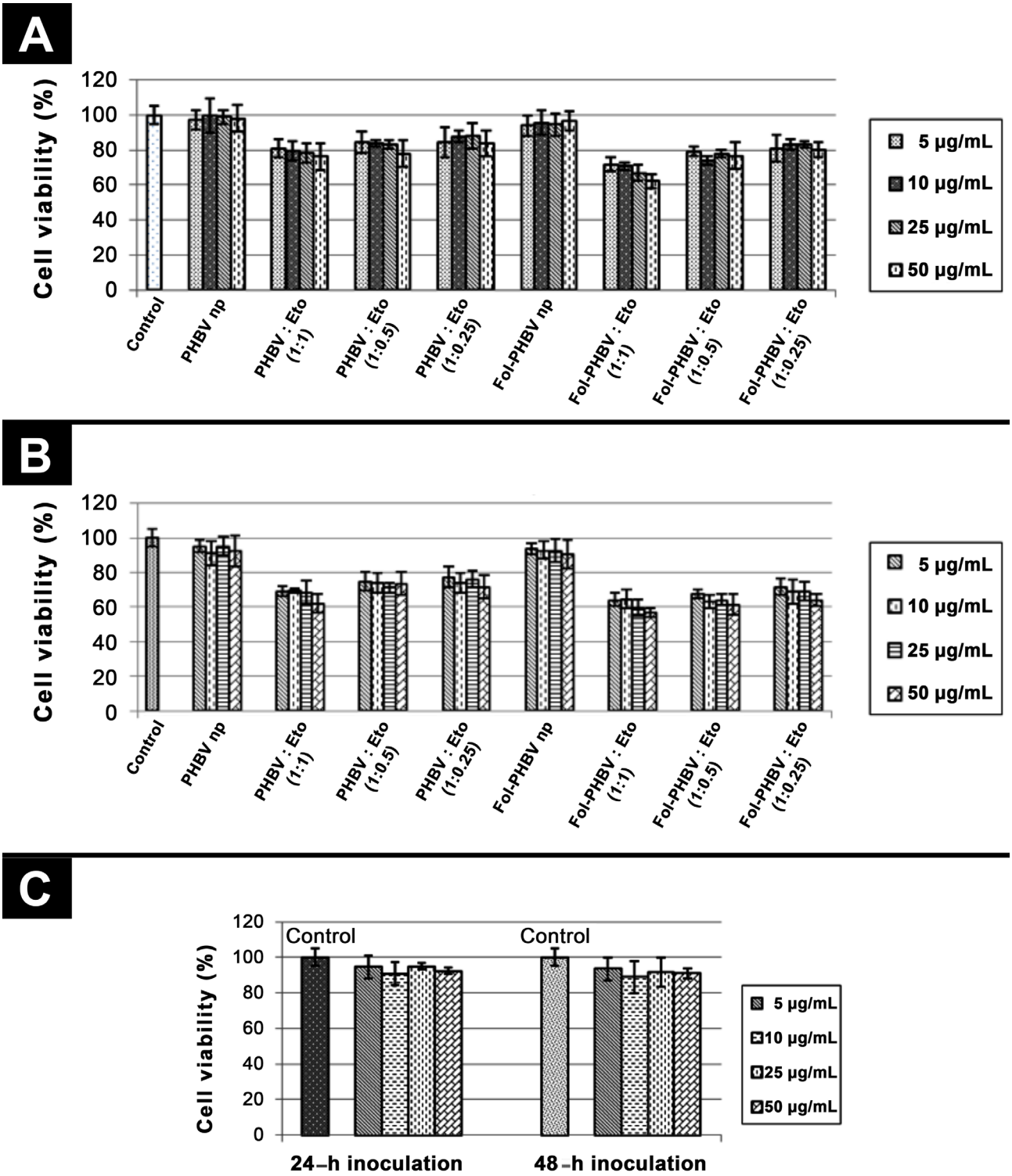

Figure 4. Cytotoxicities of different formulations of PHBV nanoparticles inoculated to Saos-2 cells for (A) 24 h and (B) 48 h. (C) Cytotoxicity of pure etoposide on Saos-2 cells for 24 h and 48 h.

3.4. Apoptosis/necrosis assay

The apoptogenic properties of nanoparticle formulations were investigated through morphological changes in saos-2 cells. Cell shrinkage, membrane blebbing, chromatin cleavage, nuclear condensation, and formation of pyknotic bodies of condensed chromatin are the typical common

features of apoptotic cells (Moongkarndi et al., 2004). In the present study, apoptosis was assayed cytologically using the double-staining methods of Hoechst–propidium iodide and Annexin V–propidium iodide. Morphological changes in cell nuclei were observed by inverted fluorescence microscope. The percentages of apoptotic and necrotic cells were also determined.

The blue fluorescent Hoechst 33342 nucleic acid stain is a cell permeable dye usually used to identify chromatin condensation and fragmentation by staining the condensed pyknotic nuclei in apoptotic cells. Propidium iodide is a DNA-binding dye that can only stain cells with increased plasma membrane permeability and loss of plasma membrane integrity. In late apoptotic and necrotic cells, the integrity of the plasma and nuclear membranes decreases, allowing propidium iodide to pass through the membranes and display red fluorescence. Apoptosis is accompanied by a change in plasma membrane structure by surface exposure of phosphatidylserine. Translocation, and in turn apoptosis, can be detected by its affinity for Annexin V, a phospholipid-binding protein (van Engeland et al., 1998). Therefore, using Annexin V in combination with propidium iodide detects apoptotic cells and discriminates between apoptosis and necrosis. The percentages of apoptotic cells (apoptotic index) obtained by Hoechst–propidium iodide and Annexin V–propidium iodide staining methods were obtained in parallel and are given in Table 3. Microscopic analysis of apoptotic cells under inverted fluorescent microscope is shown in Figures 5–7. Apoptotic cell photographs obtained from double staining with Hoechst 33342 and propidium iodide are shown in Figure 5. The morphological observation in the cell nuclei of Saos-2 cells after treatment with tested compounds showed significant morphological alterations when compared to the control. As observed in Figure 5A, untreated cells exhibited no difference in cell nuclei, with a less bright blue fluorescence due to Hoechst dye. On the other hand, cells treated with etoposide, untargeted etoposide-loaded nanoparticles, and folic-acid–conjugated etoposide-loaded nanoparticles exhibited decomposed nuclei and were brighter blue compared to untreated cells (Figures 5B–5D).

As seen in Table 3, apoptotic effect was low at low concentrations of etoposide. However, apoptotic effect increased with higher drug concentrations. The same result was also observed for drug-loaded nanoparticles as well as drug-loaded nanoparticles targeted by folic acid. A significant increase in cell apoptosis was observed in cells treated with folic-acid–conjugated, etoposide-loaded PHBV nanoparticles compared to free drug, suggesting that folic acid conjugation facilitated the incorporation of etoposide into Saos-2 cells. The highest percentage of apoptosis was obtained in cells treated with targeted nanoparticles having a 1/1 polymer/drug ratio. According to the results, the apoptotic index rose by 1%–2% when etoposide was loaded into PHBV nanoparticles. When folic acid was conjugated to drug-loaded nanoparticles, the apoptotic effect increased by 10 ± 2% with respect to the drug alone and by 8 ± 2% with respect to nontargeted drug-loaded nanoparticles. Figures 6A, 6C, and 6E reveal little green coloring caused by Annexin V staining on the cell membrane, since there was low apoptosis for the cells treated with untargeted etoposide-loaded nanoparticles, while Figures 7A, 7C, and 7E show green coloring on cell membrane due to the reaction formed by Annexin V. Moreover, in Figure 7E, the effect of folic-acid–targeted particles carrying the drug in a ratio of 1/1 (50 μg/mL) and the increase in the number of cell membranes stained in green is clearly seen.

Table 3. Apoptotic (AI) and necrotic percentage indices (NI) of etoposide (Eto), nanoparticles loaded with different ratios of etoposide (PHBV-Eto), and folic-acid–targeted nanoparticles loaded with different ratios of etoposide (FA/PHBV-Eto) in an osteocarcinoma cell line. Data represent means ± SD.

	Sample amount (μg/mL)	AI (%)					NI (%)				
		0	5	10	25	50	0	5	10	25	50
Formulations	Etoposide	1 ± 1	2 ± 1	6 ± 1	9 ± 2	14 ± 1	1 ± 1	4 ± 1	8 ± 1	12 ± 2	17 ± 3
	Etoposide/PHBV (1:0.25)	1 ± 1	2 ± 1	4 ± 1	6 ± 1	8 ± 1	2 ± 1	3 ± 1	5 ± 1	12 ± 1	17 ± 1
	FA-Eto/PHBV (1:0.25)	1 ± 1	2 ± 1	6 ± 1	8 ± 2	13 ± 1	1 ± 1	1 ± 1	7 ± 1	14 ± 2	21 ± 2
	Eto/PHBV (1:0.5)	1 ± 1	5 ± 1	8 ± 1	12 ± 1	15 ± 1	1 ± 1	3 ± 1	9 ± 1	11 ± 1	15 ± 2
	FA-Eto/PHBV (1:0.5)	2 ± 1	8 ± 1	12 ± 1	18 ± 2	21 ± 2	2 ± 1	5 ± 1	13 ± 2	16 ± 2	20 ± 1
	Eto/PHBV (1:1)	2 ± 1	4 ± 1	7 ± 1	13 ± 2	15 ± 1	2 ± 1	3 ± 1	6 ± 1	12 ± 2	18 ± 1
	FA-Eto/PHBV (1:1)	1 ± 1	8 ± 1	13 ± 1	17 ± 1	24 ± 2	1 ± 1	8 ± 1	11 ± 1	19 ± 1	25 ± 2

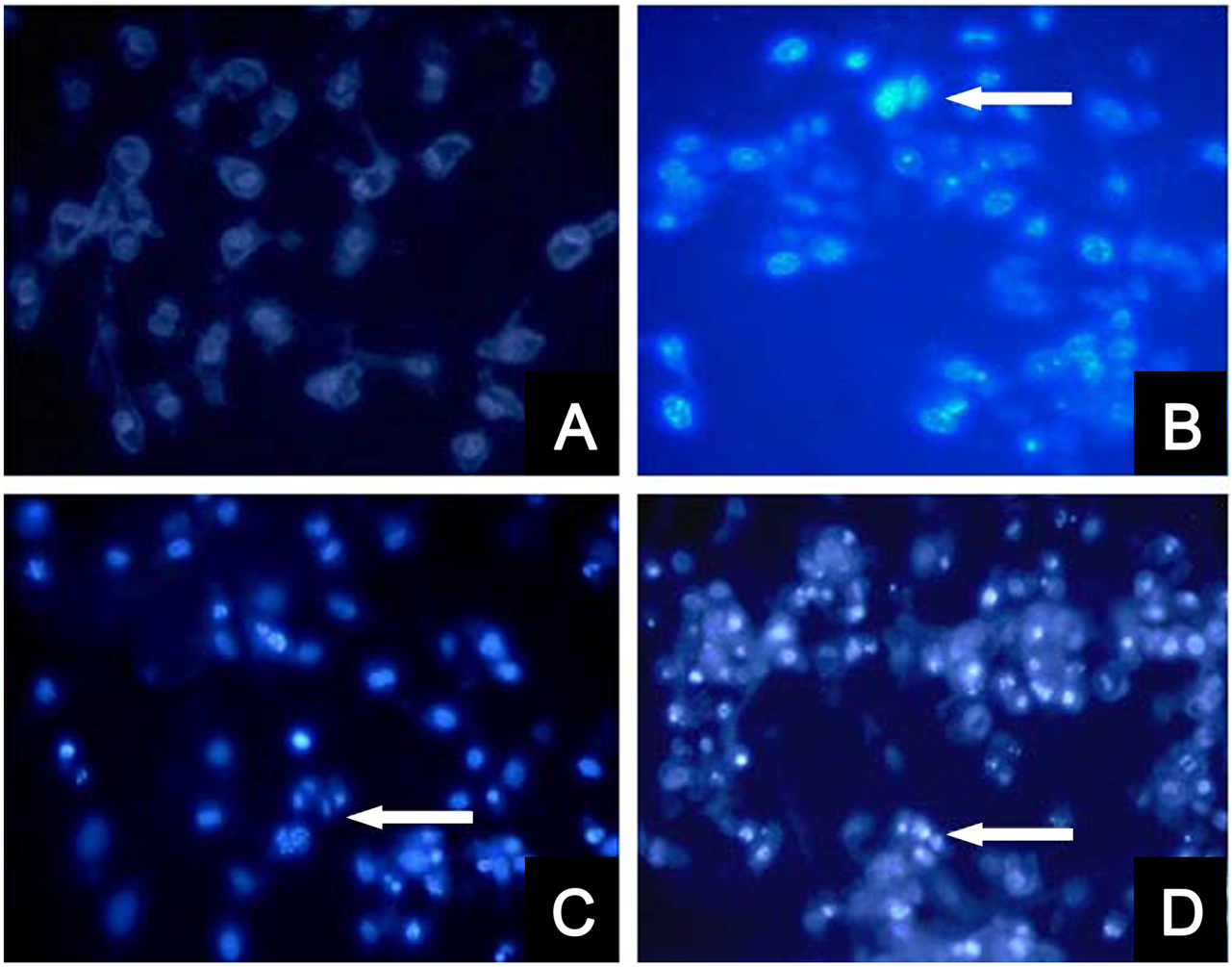

Figure 5. Apoptotic cell fluorescent photographs obtained from the Hoechst 33342/propidium iodide staining. Osteosarcoma cells (A) stained by Hoechst 33342 and not treated with drug and nanoparticles (control group), (B) interacted with NP (50 μg/mL) loaded with etoposide in the ratio of 1/0.25, (C) interacted only with etoposide (50 μg/mL), and (D) interacted with folic-acid–targeted NP (50 μg/mL) loaded with etoposide at a ratio of 1/1.

In our study, necrotic index was examined under fluorescent light (by FITC filter) at a wavelength of 480–520 nm, and at this wavelength necrotic cell nuclei were observed to be red. Healthy cells were not stained by propidium iodide and apoptotic cells were observed to be green at simultaneous times. Photographs of necrotic cells are given in Figure 8 and necrotic percentage indices are given in Table 3. As seen in Table 3, higher concentrations of the drug resulted in an increase in toxicity, and therefore, an increase in necrosis. The necrotic effect of targeted drug-loaded nanoparticles (Figures 8C and E) was found to be 8 ± 1% higher compared to cells treated with drug alone and 4 ± 1% higher compared to nontargeted drug-loaded nanoparticles. The highest necrotic index of approximately 25 ± 1% was obtained in nanoparticles targeted with folic acid at the 1/1 polymer/drug ratio and 50 μg/mL nanoparticle concentration (Figures 8E and 8F).

In conclusion, a targeted drug delivery system composed of PHBV/etoposide was successfully prepared for the treatment of osteosarcoma. The surface of nanoparticles was conjugated with folic acid to enhance the etoposide delivery to tumor cells. The nanoparticles were nanosized between 200 nm and 250 nm, depending on polymer/drug ratio and folic acid conjugation. The in vitro drug release profiles of nanoparticles exhibited a biphasic pattern, with an initial fast release followed by a slower release. Encapsulation efficiencies of nanoparticles were between 27% and 34%, depending on initial polymer/drug concentration. These characteristics, along with targeting ligand conjugation, facilitated the cellular uptake of prepared nanoparticles in Saos-2 cells. Increased cellular uptake led to the improved cytotoxic effect of targeted nanoparticles in comparison to free etoposide and nontargeted etoposide-loaded

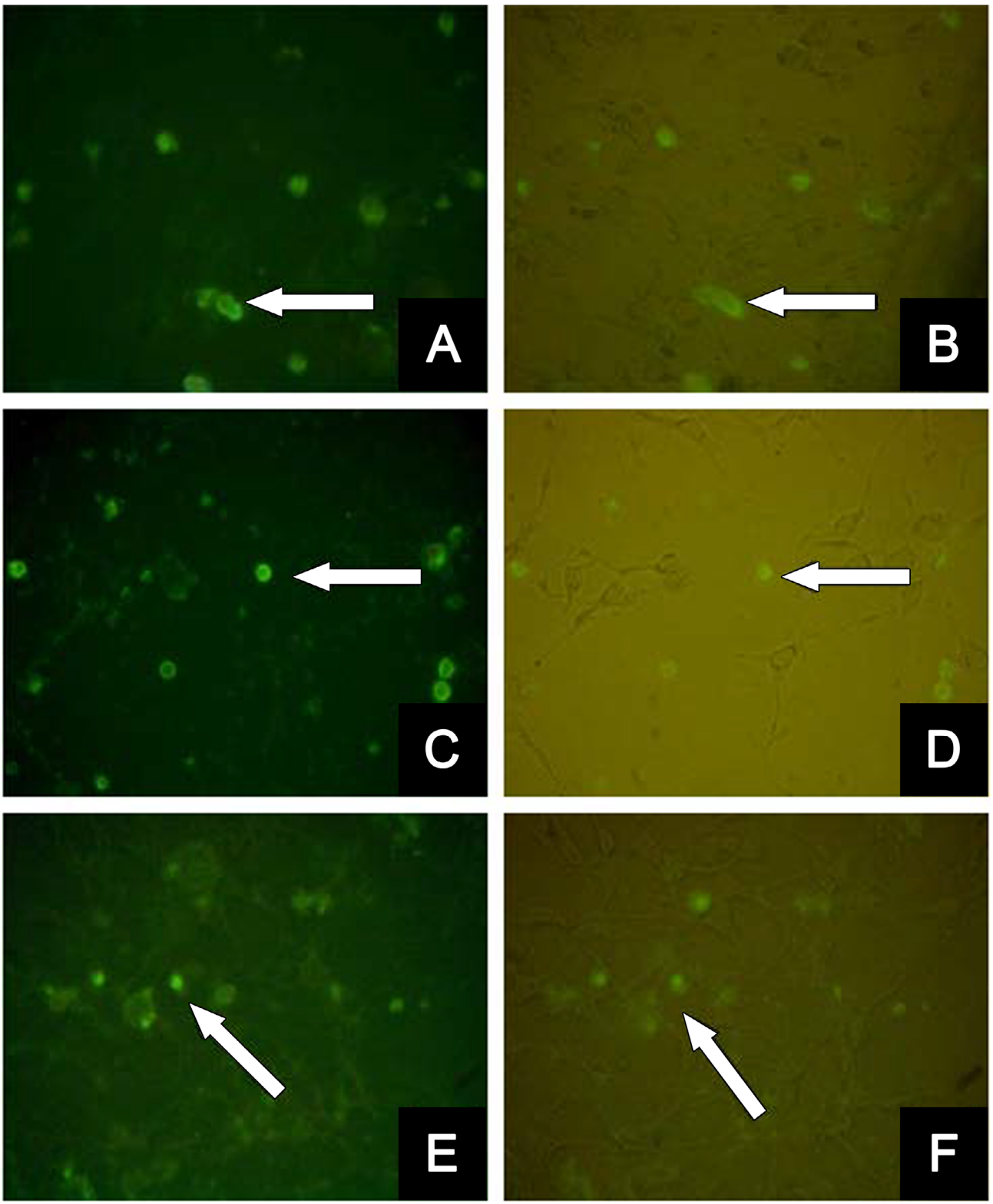

Figure 6. Apoptotic cell fluorescent photographs obtained from the Annexin V/propidium iodide staining. (A) Osteocarcinoma cells treated with untargeted nanoparticles at a polymer/drug ratio of 1/0.25 (50 μg/mL). (B) UV–Vis photo of same field. (C) Osteocarcinoma cells treated with untargeted nanoparticles at the polymer/drug ratio of 1/0.5 (50 μg/mL). (D) UV–Vis photo of same field. (E) Osteocarcinoma cells treated with untargeted nanoparticles at a polymer/drug ratio of 1/1 (50 μg/mL), (F) UV–Vis photo of same field.

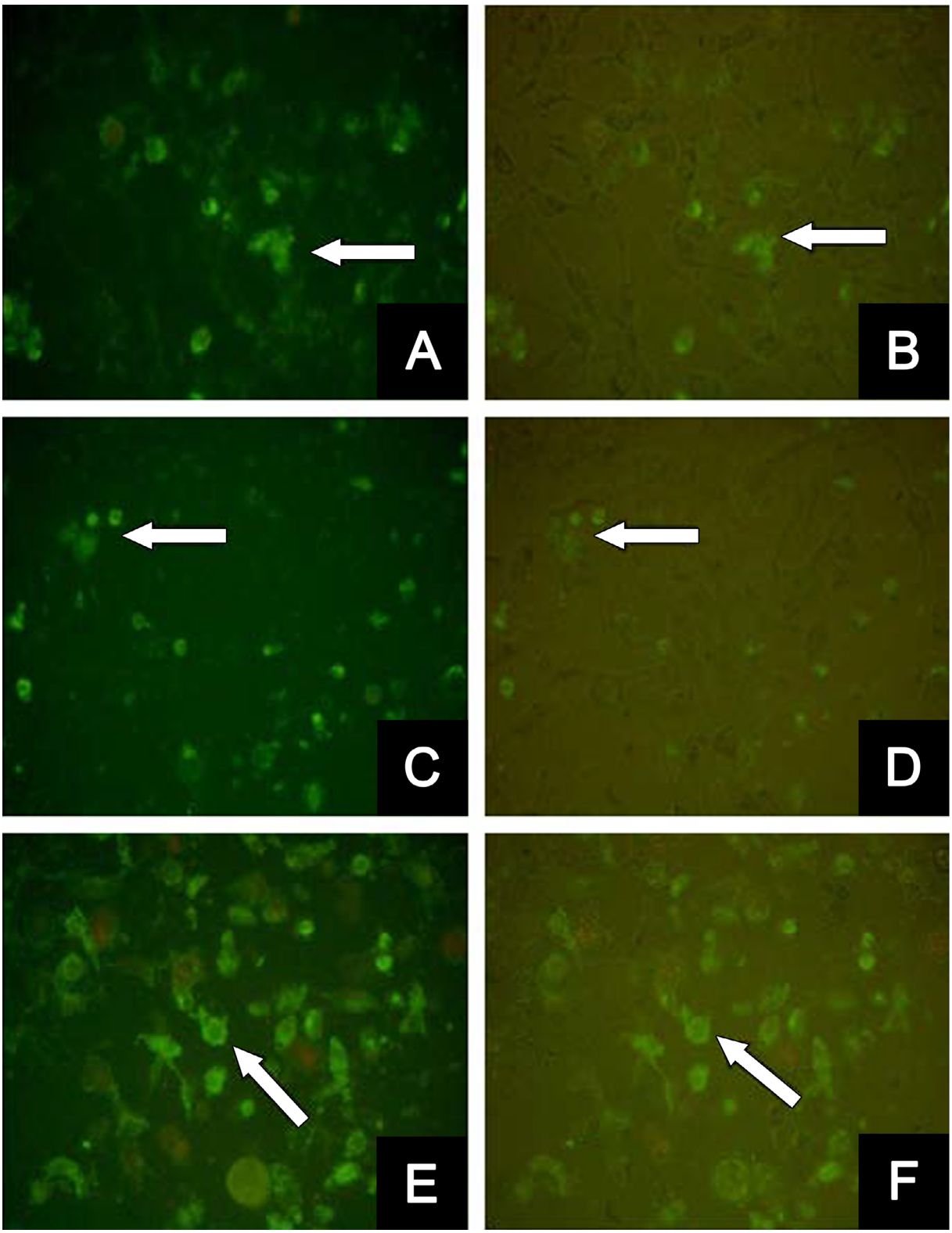

Figure 7. Apoptotic cell fluorescent photographs obtained from the Annexin V/propidium iodide staining. (A) Osteocarcinoma cells stained interacted with folic-acid–targeted NP loaded with etoposide (50 μg/mL) in a polymer/drug ratio of 1/0.25. (B) UV–Vis photo of same field. (C) Osteocarcinoma cells interacted with folic-acid–targeted NP loaded with etoposide (50 μg/mL) at a polymer/drug ratio of 1/0.5. (D) UV–Vis photo of same field. (E) Osteocarcinoma cells interacted with folic-acid–targeted NP loaded with etoposide (50 μg/mL) at a polymer/drug ratio of 1/1. (F) UV–Vis photo of same field.

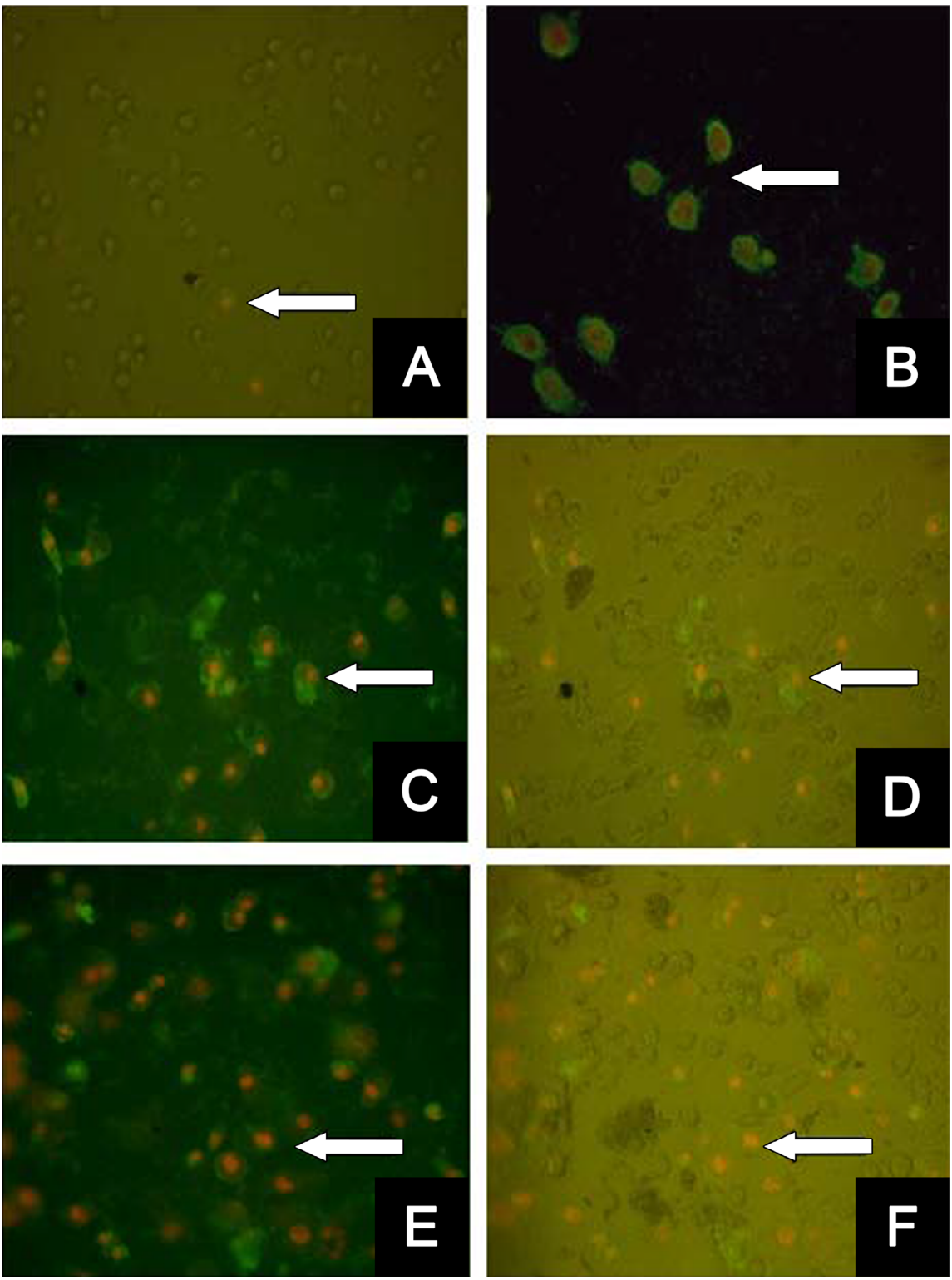

Figure 8. Necrotic cell photographs obtained from Annexin V staining performed using propidium iodide. (A) Osteocarcinoma cells stained by Annexin V staining method and not treated with drug and nanoparticles (control group). (B) Osteocarcinoma cells interacted with folic acid targeted NP loaded with etoposide (50 μg/mL) at a polymer/drug ratio of 1/1. (C) Osteocarcinoma cells interacted with folic-acid–targeted NP loaded with etoposide (50 μg/mL) at a polymer/drug ratio of 1/0.5. (D) UV–Vis photo of same field; necrotic cell nuclei look red and nonnecrotic cell nuclei look colorless. (E) Osteocarcinoma cells interacted with folic-acid–targeted NP loaded with etoposide (50 μg/mL) at a polymer/drug ratio of 1/1. (F) UV–Vis photo of same field.

nanoparticles, which is also in agreement with apoptosis/necrosis studies. These findings suggest that folic-acid–conjugated PHBV nanoparticles have potential for use as a targeted formulation of etoposide for the treatment of osteosarcoma. Further in vivo studies have been planned to demonstrate the efficacy of these nanoparticles as a targeted drug delivery system.

Acknowledgements
This study was financially supported by Hacettepe University Research Fund (Grant No. 09 01 604 001).

References

Baena-Aristizabal CM, Fessi H, Elaissari A, Mora-Huertas CE (2016). Biodegradable microparticles preparation by double emulsification-solvent extraction method: A systematic study. Colloid Surface A 492: 213-229.

Bajpai AK, Mishra A (2005). Preparation and characterization of tetracycline-loaded interpenetrating polymer networks of carboxymethyl cellulose and poly(acrylic acid): water sorption and drug release study. Polym Int 54: 1347-1356.

Decuzzi P, Ferrari M (2007). The role of specific and non-specific interactions in receptor-mediated endocytosis of nanoparticles. Biomaterials 28: 2915-2922.

Dhanaraju MD, Sathyamoorthy N, Sundar VD, Suresh C (2010). Preparation of poly (epsilon-caprolactone) microspheres containing etoposide by solvent evaporation method. Asian Journal of Pharmaceutical Science 5: 114-122.

Gassner F, Owen AJ (1996). Some properties of poly(3-hydroxybutyrate)-poly(3-hydroxyvalerate) blends. Polym Int 39: 215-219.

Hande KR (1998). Etoposide: Four decades of development of a topoisomerase II inhibitor. Eur J Cancer 34: 1514-1521.

Jabir NR, Tabrez S, Ashraf GM, Shakil S, Damanhouri GA, Kamal MA (2012). Nanotechnology-based approaches in anticancer research. Int J Nanomedicine 7: 4391-4408.

Kilicay E, Demirbilek M, Turk M, Guven E, Hazer B, Denkbas EB (2011). Preparation and characterization of poly(3-hydroxybutyrate-co-3-hydroxyhexanoate) (PHBHHX) based nanoparticles for targeted cancer therapy. Eur J Pharm Sci 44: 310-320.

Low PS, Kularatne SA (2009). Folate-targeted therapeutic and imaging agents for cancer. Curr Opin Chem Biol 13: 256-262.

Lu XY, Zhang YL, Wang L (2010). Preparation and in vitro drug-release behavior of 5-fluorouracil-loaded poly(hydroxybutyrate-co-hydroxyhexanoate) nanoparticles and microparticles. J Appl Polym Sci 116: 2944-2950.

Moongkarndi P, Kosem N, Kaslungka S, Luanratana O, Pongpan N, Neungton N (2004). Antiproliferation, antioxidation and induction of apoptosis by *Garcinia mangostana* (mangosteen) on SKBR3 human breast cancer cell line. J Ethnopharmacol 90: 161-166.

Park EK, Lee SB, Lee YM (2005). Preparation and characterization of methoxy poly(ethylene glycol)/poly(epsilon-caprolactone) amphiphilic block copolymeric nanospheres for tumor-specific folate-mediated targeting of anticancer drugs. Biomaterials 26: 1053-1061.

Parveen S, Sahoo SK (2008). Polymeric nanoparticles for cancer therapy. J Drug Target 16: 108-123.

Patil S, Sandberg A, Heckert E, Self W, Seal S (2007). Protein adsorption and cellular uptake of cerium oxide nanoparticles as a function of zeta potential. Biomaterials 28: 4600-4607.

Qian C, McClements DJ (2011). Formation of nanoemulsions stabilized by model food-grade emulsifiers using high-pressure homogenization: Factors affecting particle size. Food Hydrocolloid 25: 1000-1008.

Schwartz CL, Garlick R, Teot L, Krailo M, Chen ZJ, Goorin A, Grier HE, Bernstein ML, Meyers P (2007). Multiple drug resistance in osteogenic sarcoma: INT0133 from the Children's Oncology Group. J Clin Oncol 25: 2057-2062.

Tan CP, Nakajima M (2005). Beta-carotene nanodispersions: preparation, characterization and stability evaluation. Food Chem 92: 661-671.

Tcholakova S, Denkov ND, Sidzhakova D, Ivanov IB, Campbell B (2003). Interrelation between drop size and protein adsorption at various emulsification conditions. Langmuir 19: 5640-5649.

van Engeland M, Nieland LJW, Ramaekers FCS, Schutte B, Reutelingsperger CPM (1998). Annexin V-affinity assay: A review on an apoptosis detection system based on phosphatidylserine exposure. Cytometry 31: 1-9.

van Meerloo J, Kaspers GJ, Cloos J (2011). Cell sensitivity assays: the MTT assay. Methods Mol Biol 731: 237-245.

Vasir JK, Labhasetwar V (2005). Targeted drug delivery in cancer therapy. Technol Cancer Res T 4: 363-374.

Vilos C, Morales FA, Solar PA, Herrera NS, Gonzalez-Nilo FD, Aguayo DA, Mendoza HL, Comer J, Bravo ML, Gonzalez PA et al. (2013). Paclitaxel-PHBV nanoparticles and their toxicity to endometrial and primary ovarian cancer cells. Biomaterials 34: 4098-4108.

Wittig JC, Bickels J, Priebat D, Jelinek J, Kellar-Graney K, Shmookler B, Malawer MM (2002). Osteosarcoma: a multidisciplinary approach to diagnosis and treatment. Am Fam Physician 65: 1123-1132.

Xu FZ, Zhao TQ, Yang T, Dong LL, Guan XY, Cui XJ (2016). Fabrication of folic acid functionalized pH-responsive and thermosensitive magnetic chitosan microcapsules via a simple sonochemical method. Colloid Surface A 490: 22-29.

Yang R, Kolb EA, Qin J, Chou A, Sowers R, Hoang B, Healey JH, Huvos AG, Meyers PA, Gorlick R (2007). The folate receptor alpha is frequently overexpressed in osteosarcoma samples and plays a role in the uptake of the physiologic substrate 5-methyltetrahydrofolate. Clin Cancer Res 13: 2557-2567.

Yu MK, Park J, Jon S (2012). Targeting strategies for multifunctional nanoparticles in cancer imaging and therapy. Theranostics 2: 3-44.

Zhang C, Zhao LQ, Dong YF, Zhang XY, Lin J, Chen Z (2010). Folate-mediated poly(3-hydroxybutyrate-co-3-hydroxyoctanoate) nanoparticles for targeting drug delivery. Eur J Pharm Biopharm 76: 10-16.

Zhang TC, Chen JN, Zhang Y, Shen Q, Pan WS (2011). Characterization and evaluation of nanostructured lipid carrier as a vehicle for oral delivery of etoposide. Eur J Pharm Sci 43: 174-179.